Electronic Supplementary Material (ESI) for Energy & Environmental Science.

Electronic Supplementary Information

Solution-printable fullerene/TiS_2 organic/inorganic hybrids for high-performance flexible n-type thermoelectrics

Liming Wang[1], Zimeng Zhang[1], Linxiao Geng[2], Tianyu Yuan[3], Yuchen Liu[1], Juchen Guo[2], Lei Fang[3] , Jingjing Qiu[4], Shiren Wang[1]*

[1] Department of Industrial and Systems Engineering, Texas A&M University, College Station, Texas 77843, USA.

[2] Department of Chemical and Environmental Engineering, University of California, Riverside, California 92521, USA

[3] Department of Chemistry, Texas A&M University, College Station, Texas 77843, USA

[4]Department of Mechanical Engineering, Texas Tech University, Lubbock, TX77409, USA

*e-mail: s.wang@tamu.edu

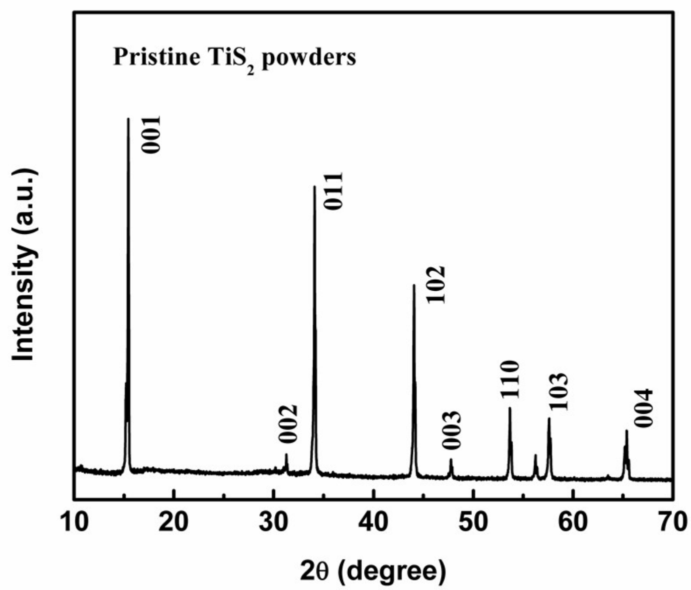

Fig. S1 The XRD pattern of pristine TiS_2 powders. All peaks match those in the reference PDF# 15-853[1,2].

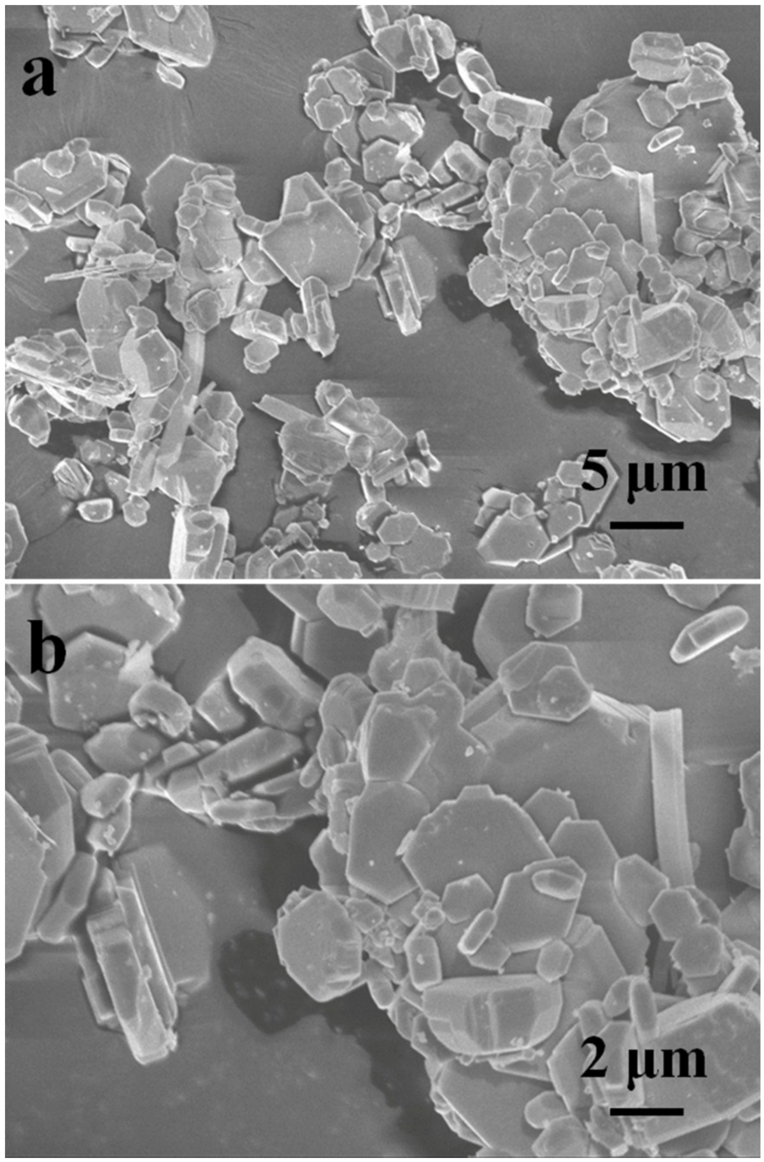

Fig. S2 The SEM images of pristine layered TiS_2 powders under different magnifications.

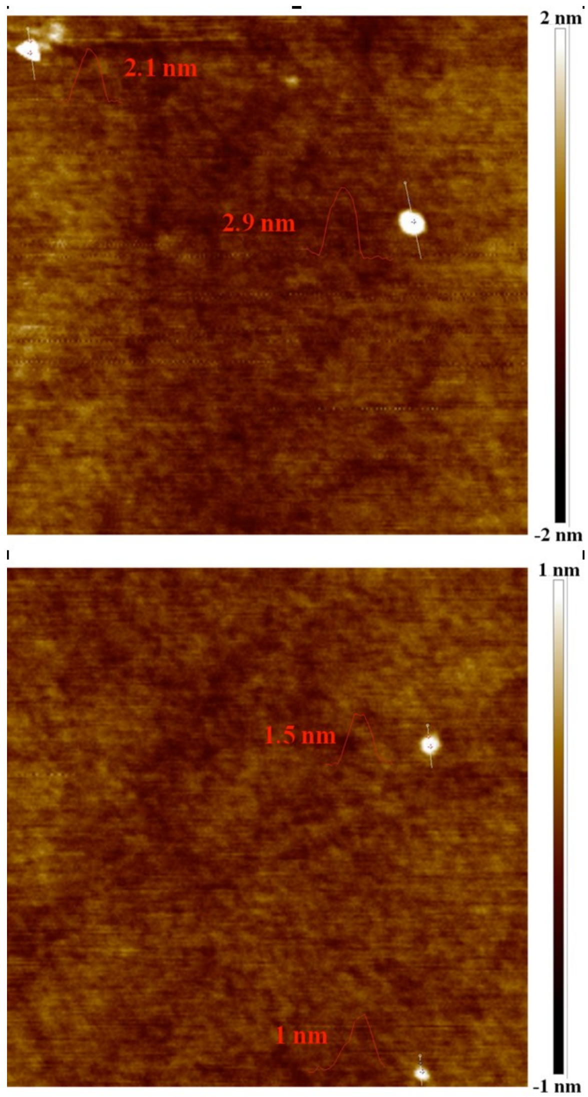

Fig. S3 The AFM images of exfoliated TiS_2 nanosheets. The testing area is 3 μm × 3 μm.

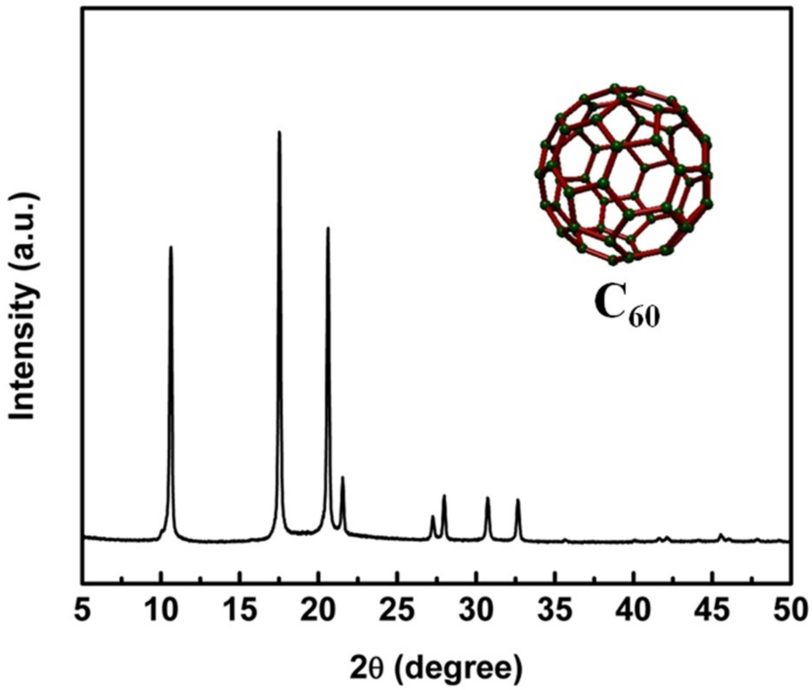

Fig. S4 The XRD pattern of pristine C_{60} powders. The peaks are consistent with previous paper.[3]

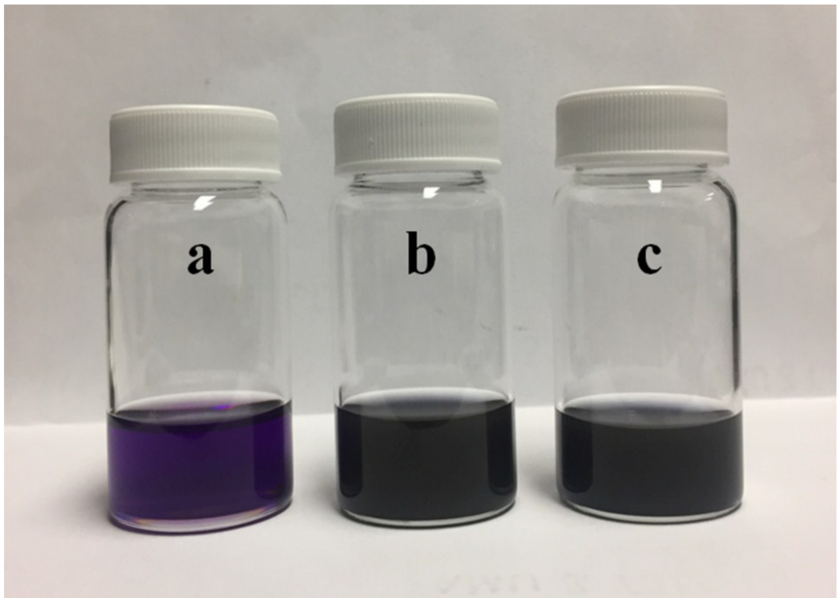

Fig. S5 The digital image of (a) 1 mg mL^{-1} C_{60}/toluene solution, (b) TiS_2 nanosheets in IPA, and (c) 1 wt% C_{60}/TiS_2 hybrids in IPA. All the solutions are very stable even after placing for one week.

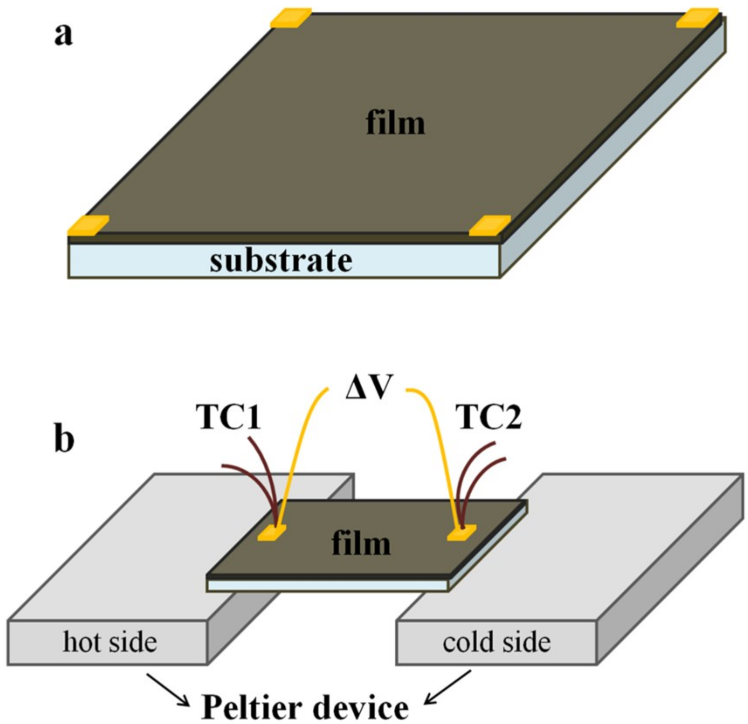

Fig. S6 (a) The sample configuration for the measurement of electrical conductivity. The electrical conductivity was measured based on the Van der Pauw method with a home-made apparatus. Electrodes were made by thermally evaporating gold on four corners of the film. Four probes were pressed on the electrodes. I-V sweep was performed using a Keithley 6221 as constant current source and a Keithley 2182A as voltage meter. The electrical conductivity measurement was calibrated with a standard resistance of 200 Ω. (b) The illustration of experimental setup for the measurements of Seebeck coefficient. In detail, peltier devices were used to create temperature difference between the two sides of thin film. Two micro-thermocouples were placed on the sample to determine the temperature difference, while two metal probes were used to record the thermoelectric voltage. The Seebeck coefficient was derived by a linear fit to the measured thermoelectric voltage versus temperature. The Seebeck coefficient of constantan was measured for calibration.

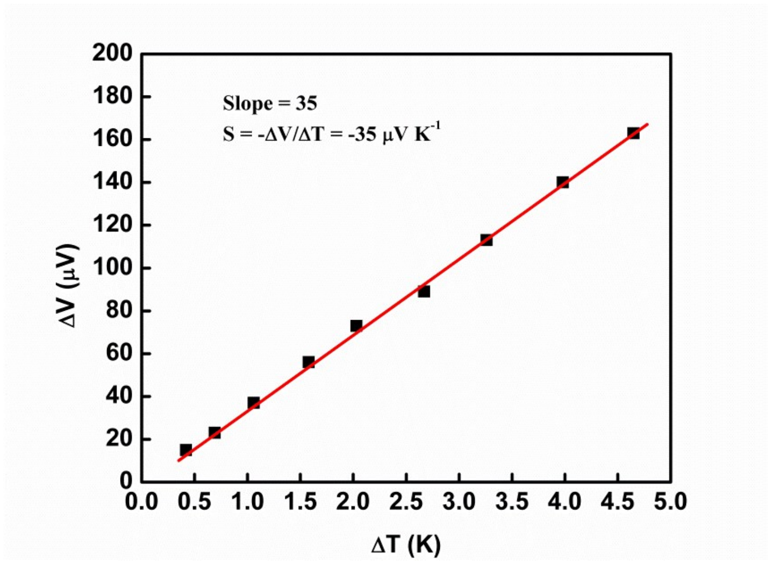

Fig. S7 Seebeck coefficient measurement curve of constantan for calibration.

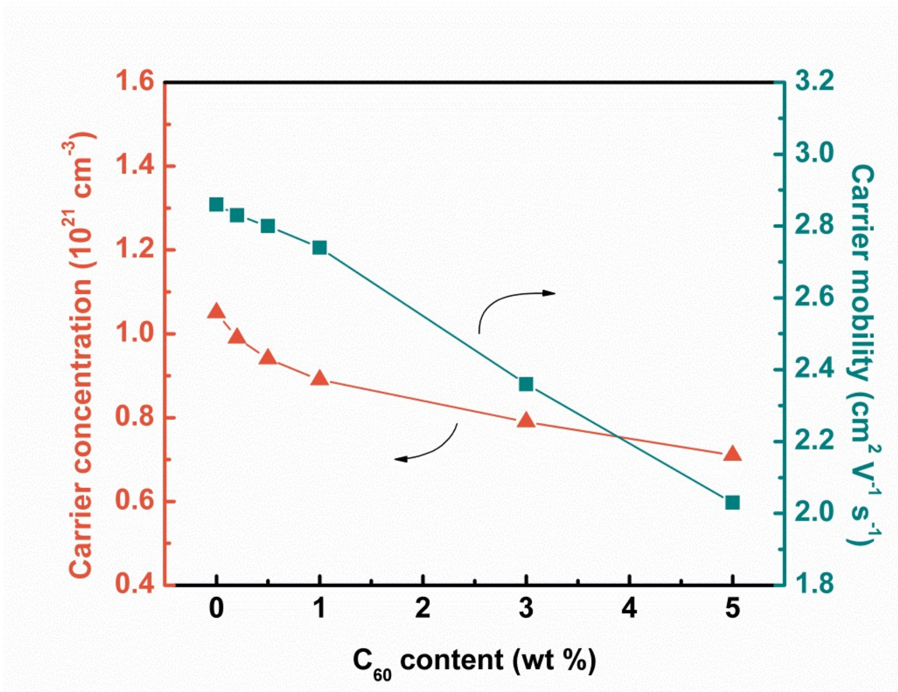

Fig. S8 The carrier concentration and carrier mobility of C_{60}/TiS_2 hybrid films as a function of C_{60} content.

The dominant scattering mechanism of TiS_2 is acoustic phonon scattering, so the scattering factor r = -1/2. The reduced Fermi energy η should be derived from the measured Seebeck coefficients,

$$S = \pm \frac{k_B}{e}\left(\frac{(r+5/2)F_{(r+3/2)}(\eta)}{(r+3/2)F_{(r+1/2)}(\eta)} - \eta\right), \qquad \text{(S1)}$$

where $F_n(\eta)$ is the n^{th}-order Fermi integral,

$$F_n(\eta) = \int_0^\infty \frac{\chi^n}{1+e^{\chi-\eta}}\,d\chi, \qquad \text{(S2)}$$

where k_B is the Boltzmann constant and e is the electron charge. The carrier effective mass (m^*) is calculated from,

$$m^* = \frac{h^2}{2k_B T}\left[\frac{n_e}{4\pi F_{1/2}(\eta)}\right]^{2/3}, \qquad \text{(S3)}$$

where h is Plank constant and n_e is the carrier concentration.[4] Based on the experimental data of S and n for fabricated TiS_2 film, m^* was calculated to be ~3.9 m_0 (m_0 is the static mass of an electron). The experimental data and Pisarenko plot of Seebeck coefficient as a function of carrier concentration at room temperature were listed in Fig. S9.

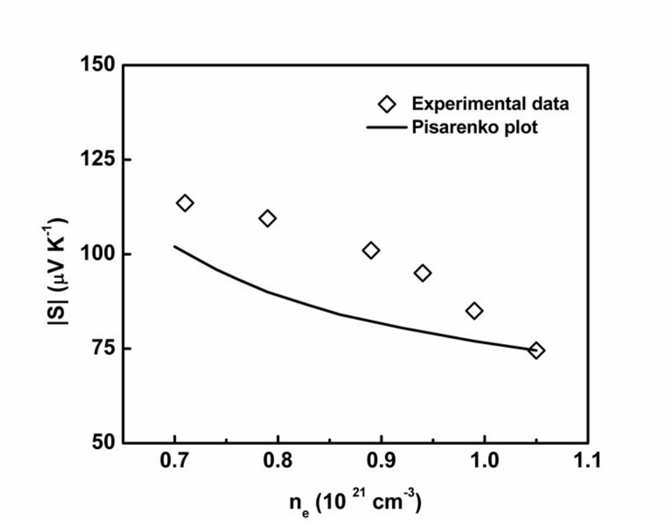

Fig. S9 The experimental Seebeck coefficient as a function of carrier concentration for fabricated films at room temperature. The solid line is the Pisarenko plot for fabricated TiS_2 film at room temperature.

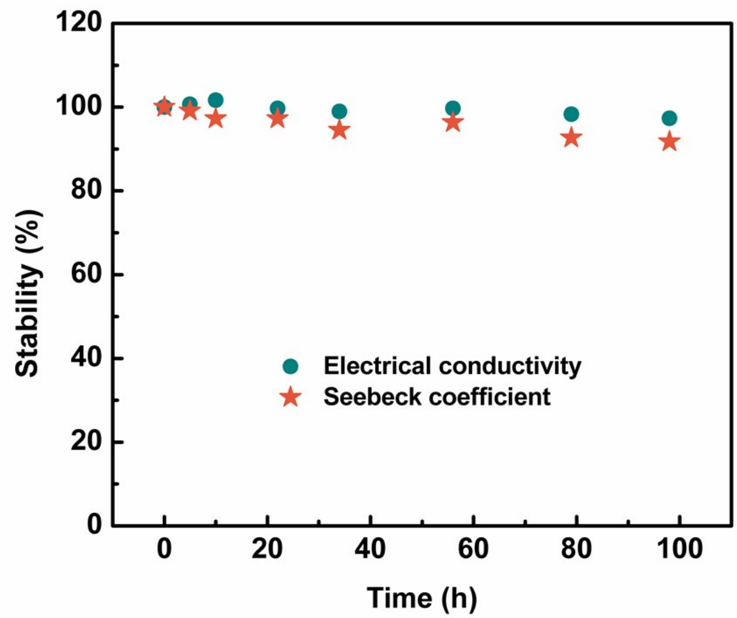

Fig. S10 Stability of 1 wt% C_{60}/TiS_2 nanosheets hybrid film.

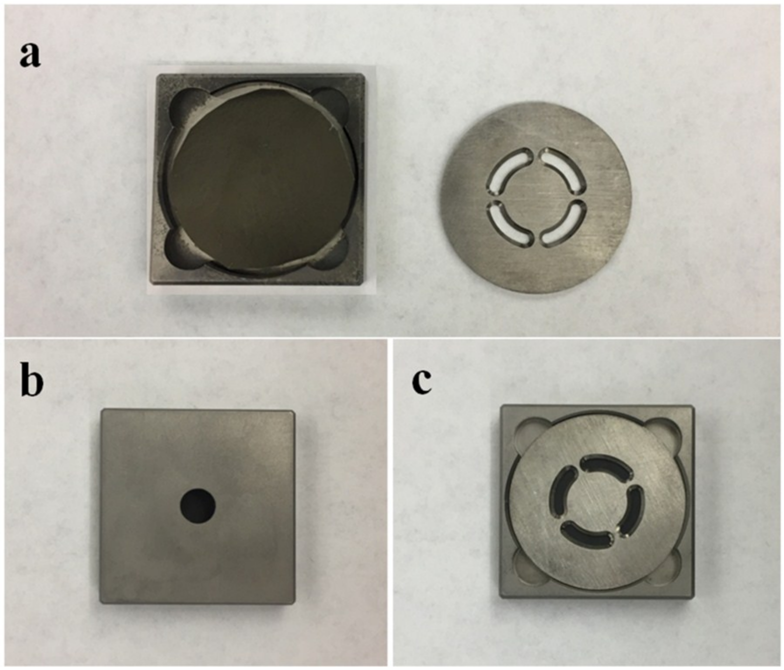

Fig. S11 (a) The digital images of special sample holder together with prepared sample for in-plane thermal conductivity measurement. (b) Bottom view. (c) Top view. The diameter of sample was around 25 mm, while the thickness was around 200-300 μm. Before test, thin graphite layers were sprayed onto each sides of the sample (exposed areas) in order to effectively absorb the laser.

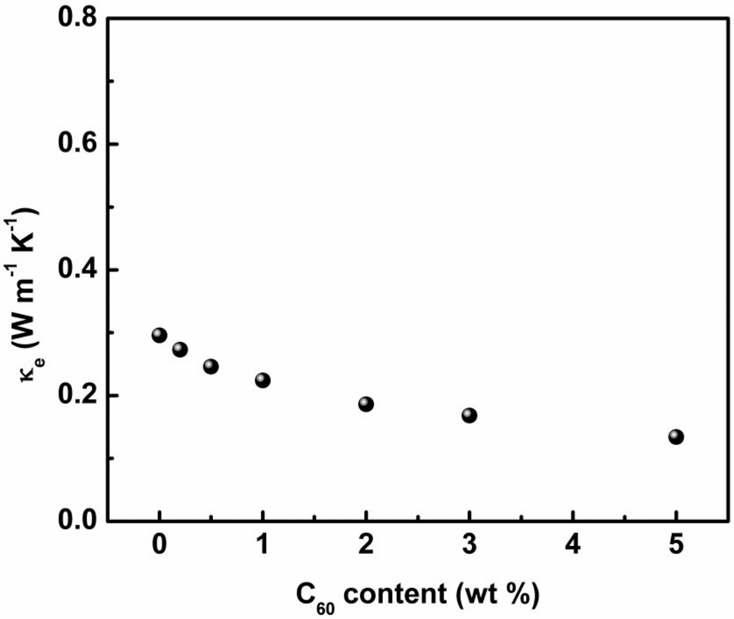

Fig. S12 The electronic thermal conductivity (κ_e) of C_{60}/TiS_2 hybrid films as a function of C_{60} content. κ_e was calculated according to the equation, $\kappa_e = L_0\sigma T$.

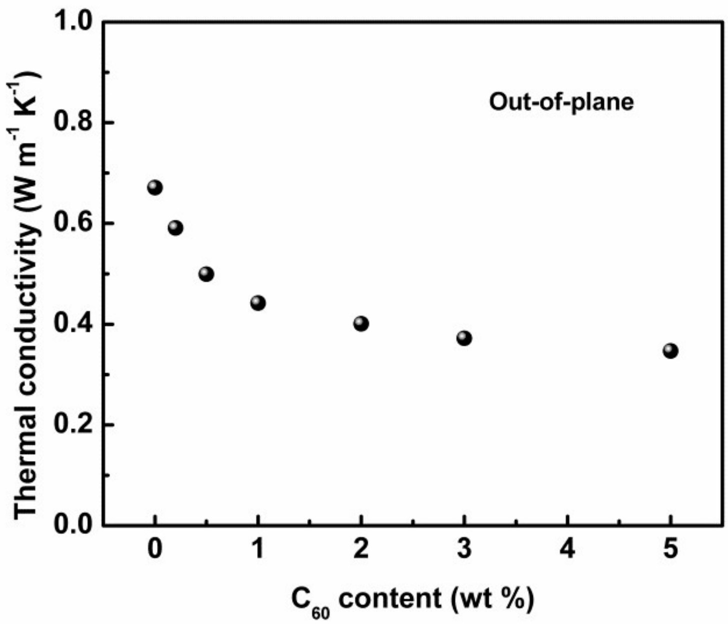

Fig. S13 Out-of-plane thermal conductivity of fabricated TiS_2 film and C_{60}/TiS_2 nanosheets hybrid films.

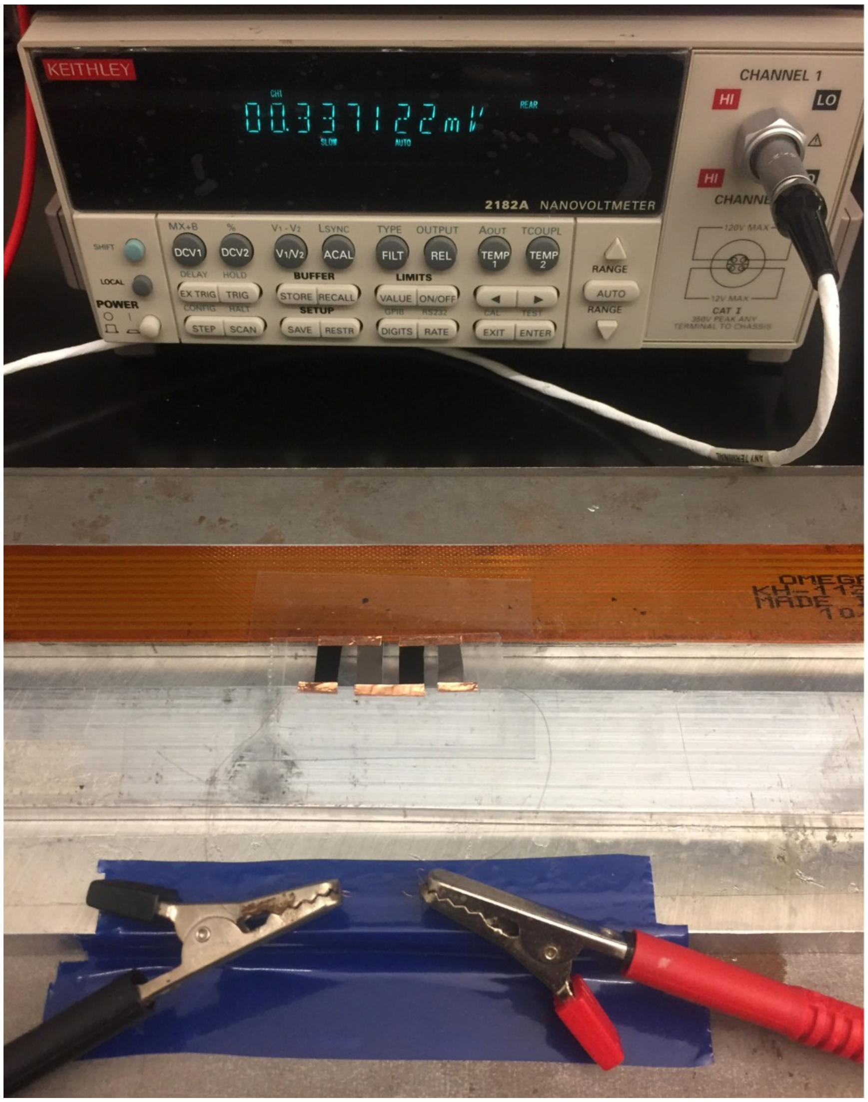

Fig. S14 Digital image of device performance measurement. Temperature difference was produced by heating one side of the device with a resistance heater, meanwhile a voltage meter (Keithley 2182A) was used to recorded the generated thermoelectric voltage.

Table S1 Calculated orientation factor (f) of fabricated TiS_2 film and C_{60}/TiS_2 nanosheets hybrid films from the XRD patterns using the Lotgering method.[5]

C_{60} content (wt %)	0	0.2	0.5	1	2	3	5
f	0.66	0.62	0.53	0.58	0.55	0.60	0.56

Table S2 List of solution-processed flexible n-type thermoelectric films based on TMDs polycrystals.[6-9]

Host materials	**Intercalation molecules**	**Electrical conductivity ($S\ cm^{-1}$)**	**Seebeck coefficient ($\mu V\ K^{-1}$)**	**Power factor ($\mu W\ m^{-1}\ K^{-2}$)**	**Ref.**
WS_2	n-butylithium	9	-75	5	6
MoS_2	benzyl viologen	0.0023	-360	0.03	7
TiS_2	HA, NMF	694	-55	210	8
TiS_2	HA, NMF	520	-67	230	9
TiS_2	**C_{60}**	**391**	**-101**	**399**	**Our work**

HA: hexylamine.

Table S3 Average in-plane thermal diffusivity and specific heat of fabricated TiS_2 film and C_{60}/TiS_2 nanosheets hybrid films.

C60 content (wt %)	0	0.2	0.5	1	2	3	5
Thermal diffusivity (mm2 s-1)	0.438	0.367	0.301	0.270	0.262	0.253	0.239

Specific heat (J g-1 K-1)	0.701	0.712	0.729	0.740	0.752	0.760	0.778

Table S4 In-plane thermal diffusivity and specific heat of fabricated TiS_2 film and 1 wt% C_{60}/TiS_2 nanosheets hybrid films as a function of temperature.

	Temperature (K)	300	320	340	360	380	400
TiS_2	Thermal diffusivity (mm^2 s^{-1})	0.438	0.433	0.426	0.412	0.397	0.397
	Specific heat (J g^{-1} K^{-1})	0.701	0.713	0.722	0.733	0.739	0.746
1 wt%	Thermal diffusivity (mm^2 s^{-1})	0.270	0.247	0.228	0.213	0.206	0.197
C_{60}/TiS_2	Specific heat (J g^{-1} K^{-1})	0.740	0.754	0.763	0.776	0.782	0.789

Table S5 Average density of fabricated TiS_2 film and C_{60}/TiS_2 nanosheets hybrid films.

C_{60} content (wt %)	0	0.2	0.5	1	2	3	5
Density (g cm^{-3})	3.125	3.116	3.097	3.073	3.042	3.011	2.958

Table S6 Thermoelectric properties of p-type leg and n-type leg for device performance measurement.

Type	Materials	Electrical conductivity (S cm^{-1})	Seebeck coefficient (μV K^{-1})	Power factor (μW m^{-1} K^{-2})
P	50 wt% PEDOT:PSS/SWNTs	1100	32	113
N	1 wt% C_{60}/TiS_2	391	-101	399

Supplementary references

1. Geng, L. et al. Titanium Sulfides as Intercalation-Type Cathode Materials for Rechargeable Aluminum Batteries. *ACS Appl. Mater. Interfaces* **9**, 21251-21257 (2017).
2. Sun, W. et al. "Water-in-Salt" electrolyte enabled LiMn2O4/TiS2 Lithium-ion batteries. *Electrochem. Commun.* **82**, 71-74 (2017).
3. Chai, B., Liao, X., Song, F. & Zhou, H. Fullerene modified C3N4 composites with enhanced photocatalytic activity under visible light irradiation. *Dalton Trans.* **43**, 982-989 (2014).
4. Zhang, J. et al. Thermoelectric properties of TiS2-xPbSnSe3 nanocomposites. *J. Alloys Compd.* **696**, 1342-1348 (2017).
5. Lotgering, F. K. et al. Topotactical reactions with ferrimagnetic oxides having hexagonal crystal structures-I. *J. Inorg. Nucl. Chem.* **9**, 113-123 (1959).
6. Oh, J. Y. et al. Chemically exfoliated transition metal dichalcogenide nanosheet-based wearable thermoelectric generators. *Energy Environ. Sci.* **9**, 1696-1705 (2016).
7. Jo, K., Choi, J. & Kim, H. Benzyl viologen-assisted simultaneous exfoliation and n-doping of MoS2 nanosheets via a solution process. *J. Mater. Chem. C* **5**, 5395-5401 (2017).
8. Tian, R. M. et al. A solution-processed TiS2/organic hybrid superlattice film towards flexible thermoelectric devices. *J. Mater. Chem. A* **5**, 564-570 (2017).
9. Wan, C. L. et al. Flexible thermoelectric foil for wearable energy harvesting. *Nano Energy* **30**, 840-845 (2016).